Plasma fluorination of carbon-based materials for imprint and molding lithographic applications

M. Schvartzman,[1] A. Mathur,[2] J. Hone,[2] C. Jahnes,[3] and S. J. Wind[4,a)]
[1]*Department of Chemical Engineering, Columbia University, New York, New York, 10027, USA and Nanotechnology Center for Mechanics in Regenerative Medicine, Columbia University, New York, New York 10027, USA*
[2]*Department of Mechanical Engineering, Columbia University, New York, New York, 10027, USA and Nanotechnology Center for Mechanics in Regenerative Medicine, Columbia University, New York, New York 10027, USA*
[3]*IBM T. J. Watson Research Center, Yorktown Heights, New York, 10598, USA*
[4]*Department of Applied Physics and Applied Mathematics, Columbia University, New York, New York, 10027, USA and Nanotechnology Center for Mechanics in Regenerative Medicine, Columbia University, New York, New York 10027, USA*

(Received 18 March 2008; accepted 6 May 2008; published online 14 October 2008)

Diamondlike carbon nanoimprint templates are modified by exposure to a fluorocarbon-based plasma, yielding an ultrathin layer of a fluorocarbon material on the surface which has a very low surface energy with excellent antiwear properties. We demonstrate the use of these plasma fluorinated templates to pattern features with dimensions ~20 nm and below. Furthermore, we show that this process is extendable to other carbon-based materials. Plasma fluorination can be applied directly to nanoimprint resists as well as to molds used to form elastomer stamps for microcontact printing and other applications requiring easy mold release. © *2008 American Institute of Physics*. [DOI: 10.1063/1.2944997]

Lithographic patterning by various molding processes, such as nanoimprint lithography (NIL), hot embossing, and elastomer molding, has become a widely used technique by experimentalists in fields ranging from physics to chemistry and biology. NIL,[1,2] in particular, is considered a candidate for next generation lithography technology by the semiconductor industry,[3] due to its high throughput potential and ability to achieve resolution in the 10 nm range and below.[4] In thermal NIL, a pattern is formed in a thin polymer film that has been cast on a substrate by molding it to a relief image in a rigid template (mask) under high pressure conditions and at a temperature above the glass transition temperature of the polymer. After cooling, the template is separated from the polymer, which subsequently serves as a resist stencil for deposition of a metal film or etching of the underlying substrate.

The most widely used materials for NIL templates are oxidized silicon and quartz,[5] although other materials with sufficiently high Young modulus, such as silicon nitride, nickel, and diamond, are used as well.[6] Antiadhesion properties, which are critical for separation of the template from the imprinted sample, are generally obtained by deposition of a fluorinated alkyl silane self-assembled monolayer[7–10] (SAM) with fluorocarbon tails at the outer surface (either by immersing the template into a solution containing the release agent[11] or by vapor deposition[12]). These outer fluorocarbon functional groups provide a low energy to the modified surface, with surface energies in the range of ~10 mJ/m^2.[13–15] However, failure of such SAM releasing layers has been reported for templates with sub-100 nm pitch and high aspect ratios,[16] possibly due to less than perfect film coverage at such dimensions, and their reliability over many imprint cycles has not been clearly demonstrated.[17]

The use of diamondlike carbon (DLC) as a NIL template material was first reported by Ramachandran *et al.*[18] DLC is well known for its high mechanical strength and low surface energy, and it is widely used as an antiwear coating for many applications;[19] however, its surface energy (~40 mJ/m^2) is not as low as that of fluorinated SAMs. Thus, for NIL applications, a surface modification of the template is likely still required. Nakamatsu *et al.* demonstrated that a fluorinated DLC film applied to a prepatterned Si/SiO_2 template has the requisite antiadhesion and antiwear properties for NIL applications.[20,21] However, those films, which were fluorinated during DLC deposition, were relatively thick, ~50 nm, precluding their use for patterning sub-100 nm features.

In this work, we present a process for modifying the surface of DLC films by exposure to a fluorocarbon-based plasma. Surface chemical analysis indicates that an ultrathin layer (~1 nm or less, depending on processing conditions) of a fluorocarbon material is formed on the surface which has a very low surface energy with excellent antiwear properties. We demonstrate the use of plasma fluorinated DLC NIL templates to pattern features with dimensions below 20 nm. Furthermore, we show that this process is extendable to other carbon-based materials. Plasma fluorination can be applied directly to NIL resists as well as to molds used to form elastomer stamps for microcontact printing and other applications requiring easy mold release. Figure 1 compares the process flow for (a) conventional antiadhesion coated NIL templates, (b) plasma fluorinated DLC templates, (c) plasma fluorinated resists for NIL as well as (d) molds for microcontact printing.

The DLC films for this work were formed in a parallel plate rf plasma enhanced chemical vapor deposition reactor at a temperature of 60 °C with the substrate electrode powered by the rf. Films were deposited by first sputter etching

a)Electronic mail: sw2128@columbia.edu.

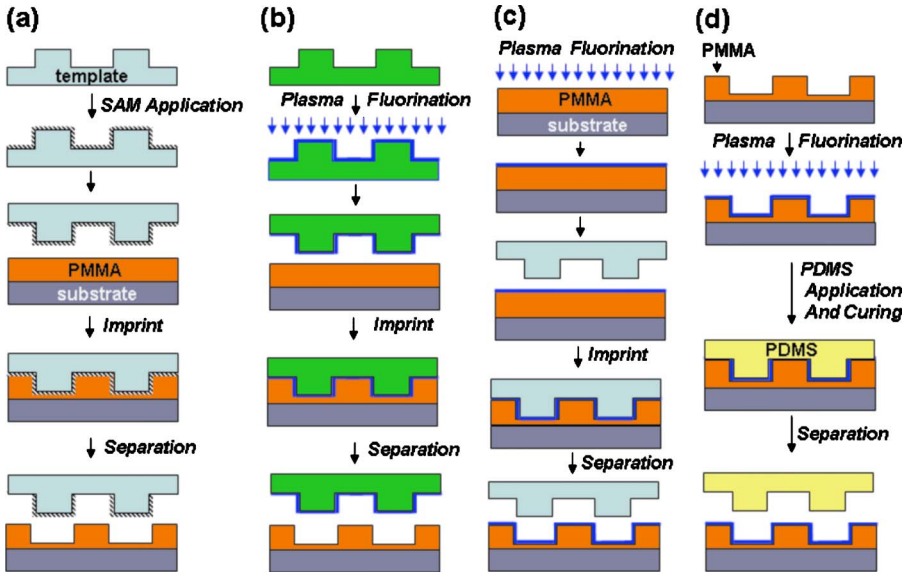

FIG. 1. (Color online) Schematic process flows for different imprint techniques: (a) nanoimprint template coated with a fluorinated SAM prior the imprint; (b) nanoimprint template subjected to a plasma-assisted surface fluorination prior the imprint; (c) imprint resist subjected to a plasma-assisted surface fluorination, while the template remains untreated; (d) a template for microcontact printing is subjected to a plasma-assisted surface fluorination prior the elastomer application.

the silicon wafer in an Ar plasma at 100 mTorr and 125 W for 30 s. The 100 nm thick DLC films were deposited using pure cyclohexane at 100 mTorr and 200 W, with a growth rate of 3.4 nm/s. Plasma fluorination was performed in an Oxford PlasmaLab 80 Plus etching system at room temperature, using C_4F_8 and CHF_3 gases. The background pressure was in the range of ~33–88 mTorr, with a gas flow rate of 100 SCCM (SCCM denotes cubic centimeter per minute at STP) and rf power of 100–300 W. Samples were exposed to the plasma for 30 s for all experiments in this work.

After exposure to the plasma, the films were characterized by a variety of techniques. A slight reduction in the DLC thickness, ~0–8 nm, was observed by ellipsometry for both C_4F_8 and CHF_3 plasmas, depending on plasma conditions, with the thickness reduction generally increasing with increasing rf power. However, samples treated by C_4F_8 at a pressure of 88 mTorr showed an additional layer of material less than 3 nm thick. The surface roughness of untreated DLC films, as characterized by atomic force microscopy, was relatively small, with a root mean square (rms) value of 0.72 nm. Oxygen plasma etching was found to reduce the rms roughness to 0.18 nm. A standard fluorination process selected for nanoimprint template fabrication (C_4F_8 plasma, 88 mTorr, rf power=100 W) increased the rms roughness of the O_2-etched DLC to ~0.45 nm.

Goniometric contact angle measurements using water and glycerol were performed in order to assess the film wetting properties. Also measured for comparison were the SiO_2 films treated with a commercial monolayer template release agent typically used for NIL templates (Nanonex NXT-100). Figure 2 shows the change in the advancing contact angle of water and glycerol, respectively, following the plasma treatment with C_4F_8 and CHF_3, for several different plasma process parameters. Contact angles of ~90°–100° were obtained for water and ~80°–85° for glycerol. Based on these measurements, surface energies in the range of ~17.6–28.8 mJ/m^2 were calculated, using the two-liquid geometric method[22,23] and two-liquid harmonic method.[24] These figures compare quite well to those measured for SAM-coated SiO_2 surfaces, which had contact angles of 87° and 78° for water and glycerol, respectively, and surface energies ~24–27.5 mJ/m^2. X-ray photoelectron spectroscopy (XPS) analysis found a significant presence of fluorine within ~9 nm of the surface of the treated samples. Elemental quantification versus depth yields the carbon/fluorine ratio shown in Table I. It can be seen that for the lower pressure samples, the fluorine content diminishes with increasing depth, while for the 88 mTorr sample, the C/F ratio remains approximately constant, suggesting a thicker fluorine-containing layer. Further analysis found that the plasma-treated samples all had contributions due to C-F, CF_2, CF_3, with C-F being the largest contribution. The thicknesses of the fluorine-containing layers, calculated from the data from three take-off angle measurements (0°, 40°, and 70°) and using a value of the mean free path of diamond, were 0.51, 0.72, and 2.84 nm for the 33, 60, and 88 mTorr samples, respectively.

DLC NIL templates were patterned by electron beam lithography using hydrogen silsequioxane[25] as a resist. The pattern was transferred into the DLC film by reactive ion

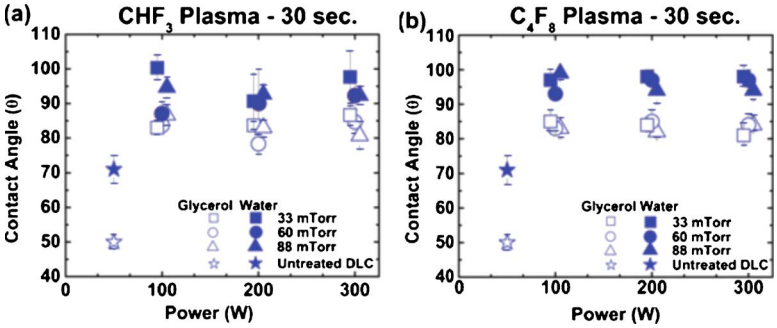

FIG. 2. (Color online) Water and glycerol contact angles after plasma fluorination using CHF_3 (a) and C_4F_8 (b), as a function of rf discharge power, for different values of the chamber pressure.

TABLE I. Carbon/fluorine ratio vs depth (C_4F_8 plasma, 200 W).

	2–3 nm	4.6–7 nm	6–9 nm
33 mTorr	1.21	1.59	1.65
60 mTorr	1.01	1.2	1.26
88 mTorr	0.7	0.64	0.58

etching in O_2 to form structures with a height of ~50 nm, followed by exposure to the fluorocarbon-based plasma. The pattern comprised arrays of small (~15 nm) dots separated by distances from 100 to 200 nm covering an area several microns in size and surrounded by larger scale features spanning a few hundred microns with a total area of several mm^2. Thermal NIL was performed at 180 °C and 500 psi using polymethyl methocrylate (PMMA) (M_W=35 K) as an imprint resist. Figure 3 shows a pattern of ~15 nm dots patterned in PMMA using this template, which was found to be extremely robust, withstanding more than 100 imprints without failure. In contrast, untreated templates suffered resist adhesion after the initial imprint.

We have found that plasma fluorination can be used not only on NIL templates but on the imprint resist as well. PMMA films that have been exposed to a C_4F_8 plasma can be imprinted and separated from untreated templates (either DLC or SiO_2). Without any plasma treatment, the PMMA had a water contact angle of 75°, whereas after the treatment the contact angle was in the range of 85°–90°. While it may be somewhat inefficient to treat each imprint substrate in this way, it does provide an alternative when antiadhesion templates are not available. Similarly, we have used fluorinated resist films as molds for microcontact printing, enabling easy separation of the elastomer. Figure 4 shows an array of fences formed in PDMS using a plasma fluorinated PMMA mold with a height of ~5 μm and an aspect ratio of 5:1. Without the fluorine treatment, it is difficult to remove the PMDS from the mold.

In conclusion, we have developed a technique for forming an ultrathin fluorinated surface layer on carbon based lithographic template materials by exposure to a fluorocarbon plasma. This layer has very low surface energy, and it is quite robust, making it suitable as an antiadhesion, antwear surface for a variety of lithographic molding applications.

The authors thank Dr. Kateryna Artyushkova at the University of New Mexico for assistance with XPS measurements and analysis. This work was supported by the National Institutes of Health through the NIH Roadmap for Medical Research under Award No. PN2EY016586 and by the National Science Foundation under Award No. NSF EF-05-07086. Additional support from the Nanoscale Science and Engineering Initiative of the National Science Foundation under NSF Award No. CHE-0641523 and by the New York State Office of Science, Technology, and Academic Research (NYSTAR) is also gratefully acknowledged.

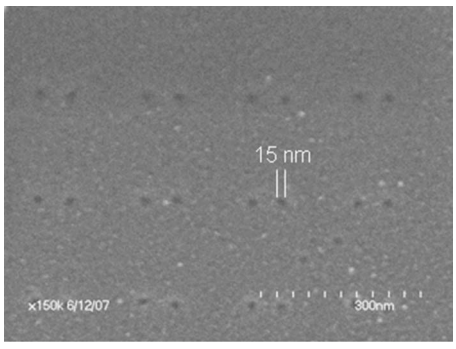

FIG. 3. Scanning electron micrograph of an array of dot pairs after NIL. The dot diameter is ~15 nm.

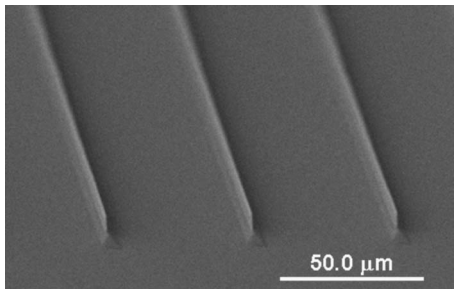

FIG. 4. Array of fences formed in PDMS using a plasma fluorinated PMMA mold. The aspect ratio is 5:1.

[1] S. Y. Chou, P. R. Krauss, and P. J. Renstrom, Appl. Phys. Lett. **67**, 3114 (1995).
[2] S. Y. Chou, P. R. Krauss, and P. J. Renstrom, Science **272**, 85 (1996).
[3] International Technology Roadmap for Semiconductors, 2005.
[4] S. Y. Chou, P. R. Krauss, W. Zhang, L. J. Guo, and L. Zhuang, J. Vac. Sci. Technol. B **15**, 2897 (1997).
[5] L. J. Guo, J. Phys. D **37**, R123 (2004).
[6] L. J. Guo, Adv. Mater. (Weinheim, Ger.) **19**, 495 (2007).
[7] M. Beck, M. Graczyk, I. Maximov, E. L. Sarwe, T. G. I. Ling, M. Keil, and L. Montelius, Microelectron. Eng. **61**, 441 (2002).
[8] M. Colburn, S. Johnson, M. Stewart, S. Damle, T. Bailey, B. Choi, M. Wedlake, T. Michaelson, S. V. Sreenivasan, J. Ekerdt, and C. G. Willson, Proc. SPIE **3676**, 379 (1999).
[9] T. Nishino, M. Meguro, K. Nakamae, M. Matsushita, and Y. Ueda, Langmuir **15**, 4321 (1999).
[10] J. J. Dumond, H. Y. Low, and I. Rodriguez, Nanotechnology **17**, 1975 (2006).
[11] I. Junarsa and P. F. Nealey, J. Vac. Sci. Technol. B **22**, 2685 (2004).
[12] T. Zhang, B. Kobrin, M. Wanebo, R. Nowak, R. Yi, J. Chinn, M. Bender, A. Fuchs, and M. Otto, Proc. SPIE **6151**, 615117 (2006).
[13] R. S. Garidel, M. Zelsmann, P. Voisin, N. Rochat, and P. Michallon, Proc. SPIE **6517**, 65172 (2007).
[14] E. F. Hare, E. G. Shafrin, and W. A. Zisman, J. Phys. Chem. **58**, 236 (1954).
[15] E. G. Shafrin and W. A. Zisman, J. Phys. Chem. **64**, 519 (1960).
[16] G. Y. Jung, Z. Y. Li, W. Wu, Y. Chen, D. L. Olynick, S. Y. Wang, W. M. Tong, and R. S. Williams, Langmuir **21**, 1158 (2005).
[17] K. Wu, X. Wang, E. K. Kim, C. G. Willson, and J. G. Ekerdt, Langmuir **23**, 1166 (2007).
[18] S. Ramachandran, L. Tao, T. H. Lee, S. Sant, L. J. Overzet, M. J. Goeckner, M. J. Kim, G. S. Lee, and W. Hu, J. Vac. Sci. Technol. B **24**, 2993 (2006).
[19] J. Robertson, Mater. Sci. Eng., R. **37**, 129 (2002).
[20] K. Nakamatsu, N. Yamada, K. Kanda, Y. Haruyama, and S. Matsui, Jpn. J. Appl. Phys., Part 2 **45**, L954 (2006).
[21] N. Yamada, K. I. Nakamatsu, K. Kanda, Y. Haruyama, and S. Matsui, Jpn. J. Appl. Phys., Part 1 **46**, 6373 (2007).
[22] D. K. Owens and R. C. Wendt, J. Appl. Polym. Sci. **13**, 1741 (1969).
[23] D. H. Kaelble and K. C. Uy, J. Adhes. **2**, 50 (1970).
[24] S. Wu, J. Polym. Sci., Part C: Polym. Symp. **1971**, 19 (1971).
[25] H. Namatsu, Y. Takahashi, K. Yamazaki, T. Yamaguchi, M. Nagase, and K. Kurihara, J. Vac. Sci. Technol. B **16**, 69 (1998).